

See discussions, stats, and author profiles for this publication at: <https://www.researchgate.net/publication/231391422>

# Temperature Cascade Control of Distillation Columns

ARTICLE *in* INDUSTRIAL & ENGINEERING CHEMISTRY RESEARCH · FEBRUARY 1996

Impact Factor: 2.59 · DOI: 10.1021/ie940758p

---

CITATIONS

27

---

READS

251

2 AUTHORS, INCLUDING:



[Sigurd Skogestad](#)

Norwegian University of Science and Techno...

**391** PUBLICATIONS **11,151** CITATIONS

SEE PROFILE

## PROCESS DESIGN AND CONTROL

## Temperature Cascade Control of Distillation Columns

Erik A. Wolff† and Sigurd Skogestad\*

Department of Chemical Engineering, University of Trondheim, NTH, N-7034 Trondheim, Norway

This paper examines how difficult control tasks are enhanced by introducing secondary measurements, creating control cascades. Temperature is much used as secondary measurement because of cheap implementation and quick and accurate response. Distillation is often operated in this manner due to slow or lacking composition measurements, although the benefits have hardly been investigated closely, especially for multivariable control applications. We therefore use distillation as the example when quantifying improvements in interaction and disturbance rejection. We also give analytical expressions for the secondary controller gain. The improvements are reached through simple cascade operation of the control system and require no complicated estimator function.

## 1. Introduction

In most process control applications, the structural issues which precede the actual controller design are the most important. The problem of *control structure selection* involves the following decisions:

1. Selection of control objectives, actuators and measurements.
2. "Control configuration selection": Selection of controller structure (e.g., pairing of actuators for decentralized control).

Note that we define the last step as the control configuration selection, whereas the combination of the two steps is denoted the "control structure selection".

In practice, control systems are implemented in a hierarchical manner, with a regulatory ("basic") control system at the lowest level. The two main objectives for the regulatory control system are as follows:

1. Take care of control tasks where fast response is needed.
2. Make the control problem, as seen from the levels above, simple.

The higher levels in the control system may include a supervisory and optimizing control system or simply the operator. In any case, the issue of control structure selection is usually most important for regulatory control. This is because the main control objective at this level is to facilitate good operation, that is, to implement a simple control system that makes it easy for the operators to operate the plant. Thus, the control objectives are not clearly defined at this level, and since the control system should be simple, we generally want to implement decentralized SISO controllers.

Specifically, one often has extra measurements which are not particularly important to the control of the plant from an overall (or economic) point of view. However, at the regulatory control level one often uses these variables as *secondary control objectives* by closing local loops. Typically, such variables may include selected temperatures and pressures. The setpoints for these

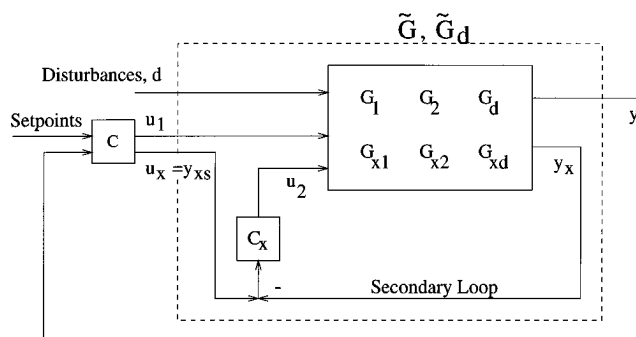


Figure 1. Block diagram with secondary loop closed.

loops may be adjusted from the higher levels, giving rise to a *cascaded control system*. Effectively, by closing secondary control loops, we replace the original independent variables (typically, flows and valve positions in process control applications) by some new independent variables (the setpoints for the secondary control variables). The idea is then that the control problem in terms of these new independent variables is simpler and at least that they need not be adjusted so frequently; that is, the "fast control" is taken care of by the secondary control loops implemented at the regulatory level.

A block diagram is shown in Figure 1. Here  $u_2$  represents the original independent variables which are used to control the secondary ("extra") outputs,  $y_x$ . After closing the secondary control loops, the setpoints for the secondary loops  $y_{xs}$  become the new control variables,  $u_x = y_{xs}$ .

Some work has been done on comparing ordinary feedback control with cascade control (see, for example, Krishnaswamey, 1990). These results mainly recommend using cascades when the deadtime in the secondary loop is much smaller than that in the primary loop.

In most practical cases it is desirable to have the secondary loops as fast as possible. Thus, when the operator or higher levels in the control system change  $u_x$ , this results in an almost immediate change in  $y_x$ , i.e.,  $y_x \approx u_x$ . Also, in this case the tuning of the secondary loops does not matter much for the overall system (provided they are sufficiently fast). However,

\* Address correspondence to this author. Fax: +47-7359-4080. E-mail: skoge@kjemi.unit.no.

† Present address: ABB Environmental, Box 6260 Etterstad, N-0603 Oslo, Norway.

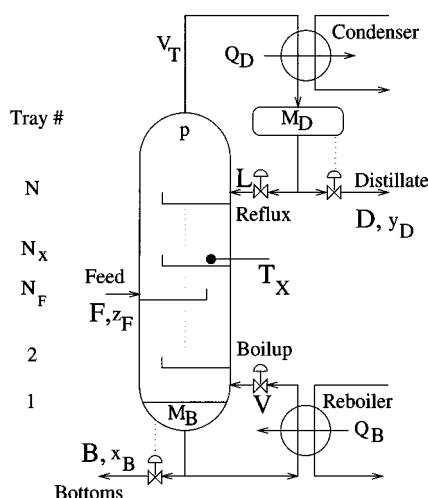


Figure 2. Typical distillation column using LV configuration.

the distillation example presented in this paper illustrates that in some cases it may be better to *not* tune the secondary loop as fast as possible and use, for example, a proportional controller in the secondary loop.

Simple proportional controllers are normally used as secondary controllers, the reason being that the primary loop will have integral action and remove stationary error anyway. In some applications PI secondary loop controllers may be beneficial, most notably when the primary loop is very slow compared to the secondary loop (e.g., Krishnaswamey and Rangaiah, 1992).

In this paper we use distillation column control as an application. The main control problem here is the strong coupling between the two loops as indicated, for example, by the large RGA values. In the paper, we study how the use of temperature cascades, in addition to improving the operation, may help reduce this interaction.

## 2. Distillation Control

Control of distillation columns is a challenging problem due to strong interactions, nonlinear behavior, and the large number of possible control structures. A simple distillation column (Figure 2) may, from a control point of view, be considered a  $5 \times 5$  problem with  $L$ ,  $V$ ,  $D$ ,  $B$ , and  $V_T$  as the manipulated inputs (actuators) and  $x_D$ ,  $x_B$  (product quality),  $M_D$ ,  $M_B$  (levels), and  $p$  (pressure) as the controlled outputs (control objectives). Typical disturbances ( $d$ ) include feed composition ( $z_F$ ), feed flowrate ( $F$ ), and feed enthalpy ( $q_F$ ).

In practice, distillation columns are usually controlled in a hierarchical manner, with the three loops for level and pressure control implemented at the regulatory control level. The "conventional" distillation control configuration selection problem, which addresses which of the five inputs should be used for control in these three loops, has been discussed by a number of authors (e.g., Shinskey, 1984; Skogestad, 1990). By convention, the resulting configuration is named by the two independent variables which are left for composition (quality) control, for example, the  $LV$  configuration uses reflux  $L$  and boilup  $V$  for composition control. In this paper the  $LV$  and  $(L/D)(V/B)$  configurations are considered.

The quality control is often implemented at some higher level or left for manual control by the operators. However, this approach has several problems:

(a) Unless very fast control is used, the use of  $u_1 = V$  and  $u_2 = L$  to control  $y_1 = x_B$  and  $y_2 = x_D$  yields a very difficult control problem with strong interactions and large RGA values.

(b) There is often a long delay associated with measuring the product compositions, which makes fast control impossible.

(c) There is a need to close at least one loop with relatively fast control in order to "stabilize" the compositions in the distillation column, which otherwise behave almost as a pure "integrator".

To deal with at least the last problem, one often implements a secondary temperature loop at the regulatory control level (e.g., Kister, 1990). This loop makes it possible for the operators to operate the column when the composition loops are not closed.

Fuentes and Luyben (1983) claim that a loosely tuned (proportional only) cascade loop is best for rejecting feed composition disturbances, while tight tuning takes best care of feed rate disturbances.

Fagervik *et al.* (1981) hold that one-way decoupling seems preferable to two-way decoupling in dual composition control. This is due to better or equal performance and less sensitivity to modeling inaccuracies.

Clarifications and extensions to these results are presented in later sections.

*Remark.* An alternative approach is to use multiple temperature measurements along the column to estimate the compositions (e.g., Mejdell and Skogestad, 1991a,b). This avoids the measurement delay and makes it easier to have fast control. However, even in this case one may for operational reasons want to close one temperature loop at the regulatory control level as described above.

## 3. Closing Secondary Loops

**3.1. General Results.** From Figure 1 we have with the secondary loops open ( $C_x = 0$ )

$$y = G_1 u_1 + G_2 u_2 + G_d d \quad (1)$$

(Note that we have assumed that some regulatory loops, e.g., the pressure and level loops for distillation columns, have been closed.) Similarly, with  $C_x \neq 0$ , the model for the secondary output is

$$y_x = G_{x1} u_1 + G_{x2} u_2 + G_{xd} d \quad (2)$$

Closing the secondary loops effectively means that we replace the inputs  $u_2$  by the setpoints  $u_x = y_{xs}$ , and for the cascaded system, we get

$$y = \tilde{G}_1 u_1 + \tilde{G}_2 u_x + \tilde{G}_d d \quad (3)$$

where

$$\tilde{G}_1 = G_1 - G_2 C_x (I + G_{x2} C_x)^{-1} G_{x1} \quad (4)$$

$$\tilde{G}_2 = G_2 C_x (I + G_{x2} C_x)^{-1} \quad (5)$$

$$\tilde{G}_d = G_d - G_2 C_x (I + G_{x2} C_x)^{-1} G_{xd} \quad (6)$$

In most cases we use decentralized control for the cascade loops and  $C_x$  is a diagonal matrix. The use of the cascade clearly changes the "effective" plant as seen from the disturbances and inputs. Specifically, if the cascade loops are slow ( $C_x \rightarrow 0$ ), we have

$$\tilde{G}_1 = G_1, \quad \tilde{G}_2 = G_2 C_x, \quad \tilde{G}_d = G_d \quad (7)$$

and as expected the system behaves as without the cascade except that the inputs  $u_2$  are scaled by  $C_x$ . At the other extreme, tight control of the secondary variables ( $C_x \rightarrow \infty$ ) yields  $G_2 C_x (I + G_{x2} C_x)^{-1} \approx G_2 G_{x2}^{-1}$  and

$$\begin{aligned}\tilde{G}_1 &= G_1 - G_2 C_{x2}^{-1} G_{x1} \\ \tilde{G}_2 &= G_2 G_{x2}^{-1} \\ \tilde{G}_d &= G_d - G_2 G_{x2}^{-1} G_{xd}\end{aligned}\quad (8)$$

The changes in control properties resulting from implementing the secondary loops may be analyzed by use of a number of standard measures for linear controllability evaluation, such as RHP zeros, RGA analysis for interactions, disturbance sensitivity, and sensitivity to model uncertainty.

**3.2. Analysis Tools.** In this paper we mainly use the relative gain array (RGA or  $\Lambda$ ) to look at interaction in the distillation column with an added temperature control loop. The properties of the RGA are well-known (e.g., Grosdidier, 1985). The most important for our purpose are (1) no two-way interaction is present when  $\Lambda = I$ , (2) the RGA is independent of scaling in inputs or outputs, and (3) the rows and columns both sum up to 1. For  $2 \times 2$  systems the RGA is especially easy to compute; because of the third property mentioned, we only have to compute the (1, 1) element of the RGA which is given by  $\lambda_{11} = 1/(1 - Y)$ , with  $Y = g_{12}g_{21}/g_{11}g_{22}$ . One deficiency of the RGA is that triangular plants (having only one-way interaction) give  $\Lambda = I$ . Hovd and Skogestad (1992) therefore introduced the performance relative gain array. The PRGA is defined as  $G_{\text{diag}} G^{-1}$ , where  $G_{\text{diag}}$  is the matrix consisting of only the diagonal elements of  $G$ . Large off-diagonal entries in the PRGA indicate significant one-way interaction.

To evaluate the disturbance sensitivity, we consider the closed-loop disturbance gain (CLDG), which is the appropriate measure when we use decentralized control (Hovd and Skogestad, 1992). The CLDG is defined as  $G_{\text{diag}} G^{-1} G_d$ , where  $G_{\text{diag}}$  consists of the diagonal elements of  $G$ .

Although the main part of the analysis is based on the RGA, we also provide detailed controller designs and simulations to confirm the predictions.

**3.3. Temperature Cascade for Distillation Column.** We here consider composition control by manipulating the reflux  $L$  and boilup  $V$  ( $LV$  configuration), but the following development also applies to other control configurations.

We use a tray temperature measurement for cascade control. Which tray to place this measurement on will be addressed in a later section. For a binary mixture with constant pressure there is a direct relationship between tray temperature ( $T$ ) and composition ( $x$ ). In terms of deviation variables we then have  $T_x = K_{Tx} x_x$ , where for ideal mixtures  $K_{Tx}$  is approximately equal to the difference in pure-component boiling points. The open-loop model for the  $LV$  configuration may be written as

$$\begin{pmatrix} x_D \\ x_B \\ x_x \end{pmatrix} = \begin{pmatrix} g_{11} & g_{12} \\ g_{21} & g_{22} \\ g_{x1} & g_{x2} \end{pmatrix} \begin{pmatrix} L \\ V \end{pmatrix} \quad (9)$$

where  $x_D$ ,  $x_B$ , and  $x_x$  are the compositions in the top, bottom, and  $x$ th tray of the distillation column. See also Figure 3 for a description of the cascade.

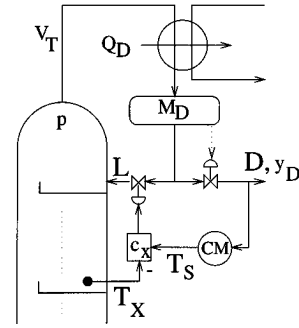


**Figure 3.** Composition control using temperature in secondary loop. CM is for composition measurement.

We now implement a SISO controller from the temperature  $T_x$  to the reflux  $L$ :  $L = c_x(T_s - T_x)$ . (we could have used boilup instead). Here  $T_s$  is the setpoint for the temperature loop which becomes the new manipulated variable instead of  $L$ . In terms of the general problem discussed above, this corresponds to selecting  $u_1 = V$ ,  $u_2 = L$ ,  $u_x = T_s$ ,  $y_x = T_x$ , and  $y = [x_B \ x_D]^T$ . We can now write the linear equations relating the top and bottom compositions to the new set of manipulated variables as

$$\begin{pmatrix} x_D \\ x_B \end{pmatrix} = \tilde{G} \begin{pmatrix} T_s \\ V \end{pmatrix} \quad (10)$$

$$\tilde{G} = \begin{pmatrix} \frac{g_{11}c_x}{1 + g_{x1}c_xK_{Tx}} & g_{12} - \frac{g_{11}g_{x2}c_xK_{Tx}}{1 + g_{x1}c_xK_{Tx}} \\ \frac{g_{21}c_x}{1 + g_{x1}c_xK_{Tx}} & g_{22} - \frac{g_{21}g_{x2}c_xK_{Tx}}{1 + g_{x1}c_xK_{Tx}} \end{pmatrix}$$

The RGA for  $\tilde{G}$  can now be computed to study the interaction properties of the column for different temperature loop gains  $c_x$ ,

$$\lambda_{11}(\tilde{G}) = \left( 1 - \frac{g_{21}g_{12} - \frac{g_{21}g_{11}g_{x2}c_xK_{Tx}}{1 + g_{x1}c_xK_{Tx}}}{g_{11}g_{22} - \frac{g_{21}g_{11}g_{x2}c_xK_{Tx}}{1 + g_{x1}c_xK_{Tx}}} \right)^{-1} \quad (11)$$

We have the two limiting cases,

$$c_x = 0: \quad \lambda_{11}(\tilde{G}) = \left( 1 - \frac{g_{12}g_{21}}{g_{11}g_{22}} \right)^{-1} = \lambda_{11}(G) \quad (12)$$

$$c_x = \infty: \quad \lambda_{11}(\tilde{G}) = \left( 1 - \frac{g_{21}(g_{12}g_{x1} - g_{11}g_{x2})}{g_{11}(g_{22}g_{x1} - g_{21}g_{x2})} \right)^{-1} \quad (13)$$

As expected, with sufficiently slow temperature cascade controllers, the RGA is unchanged.

Ideally, we would like no two-way interaction. Setting  $\lambda_{11} = 1.0$  and solving eq 11 for  $c_x$  yields the following "optimal" feedback controller,

$$c_x^* = K_{Tx}^{-1} \left( \frac{g_{12}}{g_{11}g_{x2} - g_{12}g_{x1}} \right) \quad (14)$$

The optimal loop transfer function for the temperature loop is then given by,

$$L^* = c_x^* K_{Tx} g_{x1} = - \left( 1 - \frac{g_{11}g_{x2}}{g_{12}g_{x1}} \right)^{-1} = \lambda_{11}(G^c) - 1 \quad (15)$$

where

$$G^s = \begin{pmatrix} g_{11} & g_{12} \\ g_{x1} & g_{x2} \end{pmatrix} \quad (16)$$

Thus, the optimal loop gain is essentially equal to the RGA involving  $x_D$  and  $x_x$  as outputs. Put differently, the least interaction is found when the gain around the secondary loop is near proportional to the original interaction between the top and tray  $x$  compositions. We note that, when  $x_D$  and  $x_x$  are strongly coupled (in terms of the RGA), then the loop gain should be large. This is comparable to the strong effort needed to control two measurements situated close to each other in a process.

Also, the bandwidth of the cascade loop should be approximately equal to the frequency where this "local" RGA approaches 1. This will give a system that has the power to attenuate local disturbances and will also decouple at almost all frequencies, not just at steady state. For the  $LV$  configuration the shapes of the open-loop gains (e.g.,  $g_{x1}$ ) and the RGA as a function of frequency are similar (they break off at the dominant time constant, e.g., see Skogestad (1990)). Therefore, it seems that a simple proportional controller should be close to the optimal choice. Thus, in the example below we will only consider the steady-state value of  $\lambda_{11}(\bar{G})$  and primarily assume that  $c_x$  is a P controller.

#### 4. Distillation Example

We consider as an example high-purity binary distillation. We study the system corresponding to column A studied by Skogestad and Morari (1988) with the addition of liquid flow dynamics. The basic data are given below:

no. of trays	$x_D$	$1 - x_B$	$z_F$	$L/F$	$M/F[\text{min}]$
41	0.99	0.99	0.5	2.71	0.5

We use a 82nd-order linear model in all work in this paper. The resulting liquid lag from the top to the bottom of the column is about  $\Theta_L = 1.5$  min. The steady-state RGA value of the model is  $\lambda_{11}(G) = 35.5$  and approaches 1 at frequency  $1/\Theta_L$  (also see Figure 5 with  $K_c = 0$ ).

##### 4.1. Selection of Tray for Temperature Sensor.

There are several effects that must be taken into account when choosing where to install the temperature sensor: (1) When using a secondary loop involving reflux as the input, the sensor should be placed in the top part of the column to minimize the process delay due to the liquid flow dynamics. Time delay is detrimental to performance for both SISO and MIMO cases. (2) The optimal loop gain in eq 15 will depend on secondary measurement location. This loop gain should be small enough to allow the actuator to follow suit.

Temperature differences in the top of a high-purity distillation column are very small. Using a very small  $\Delta T$  as measurement would therefore lead to equally large secondary controller gains, approaching infinity for a secondary loop based on a temperature measurement on the top tray. This gain will drop down to a value of  $\lambda_{11}(G) - 1 = 34.5$  with the measurement located at the bottom of the column. (3) The temperature measurement should be sensitive such that it may be distinguished from noise (this consideration is probably the most important). Other sources of measurement uncertainty are pressure variations (typically  $\pm 2\%$ ) and

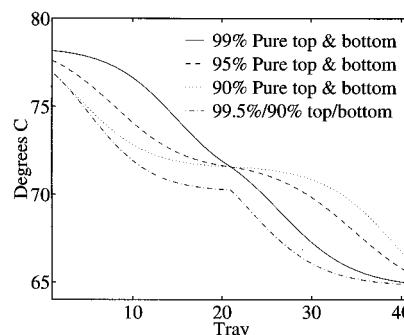


Figure 4. Steady-state column temperature profile at different operating points. (Bottom is tray 1.)

variations in content of nonproduct components in the multicomponent case. These considerations often translate to a minimum temperature sensitivity of  $1^\circ\text{C}$ .

It is important to note that the existing column profile may dictate in which end to implement a secondary measurement. This results from the column profile sometimes showing significant temperature variations in only the rectifying or stripping section depending on the design, operating point, and feed composition. See also Tolliver and McCune (1980) for a further discussion on optimum temperature control trays.

Figure 4 depicts different column temperature profiles as a function of operating conditions. To get high sensitivity (point 3 above), we have chosen to control the temperature at tray 34 (tray 8 counted from the top) for the remaining analysis.

**4.2. Controllability Analysis.** The model in eq 9 then becomes, at steady state,

$$\begin{pmatrix} x_D \\ x_B \\ x_{34} \end{pmatrix} = \begin{pmatrix} 0.8754 & -0.8618 \\ 1.0846 & -1.0982 \\ 6.3912 & -6.3051 \end{pmatrix} \begin{pmatrix} L \\ V \end{pmatrix} \quad (17)$$

We get

$$\lambda_{11}(G^s(0)) = \left(1 - \frac{g_{12}g_{x1}}{g_{11}g_{x2}}\right)^{-1} = 477.9 \quad (18)$$

and since  $K_{Tx} = -13.5$  in our example, we will have no two-way interaction at steady state, with the optimal P controller having gain

$$c_x^* = K_c = \frac{1}{K_{Tx}g_{x1}}(\lambda_{11}(G^s(0)) - 1) = \frac{476.9}{-13.5 \times 6.3912} = -5.53 \quad (19)$$

To avoid misinterpretation of "larger" and "smaller" values of  $K_c$ , we will speak of  $|K_c|$  (i.e., absolute value) in the rest of this section.

Frequency-dependent RGA plots for the column,  $\lambda(\bar{G}(j\omega))$ , with various gains for the temperature cascade are shown in Figure 5. We note that with  $K_c = 5.53$  the RGA is close to 1.0 at most frequencies (and not only at steady state). Other secondary tray placements (not shown) will show similar interaction results for varying secondary loop gain, although some placements may have an unacceptable secondary loop gain. This confirms that a simple P controller may be close to the optimal. It is interesting to note that  $\lambda_{11} = 1.0$  is not a limit, as for  $K_c > 5.53$  the interaction becomes more pronounced again with  $0 < \lambda_{11} < 1$ .

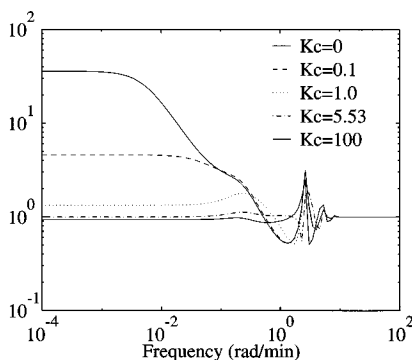


**Figure 5.** Effect on the frequency-dependent RGA,  $\lambda_{11}(\tilde{G}(j\omega))$ , of varying gain in the secondary loop,  $c_x = K_c$ .

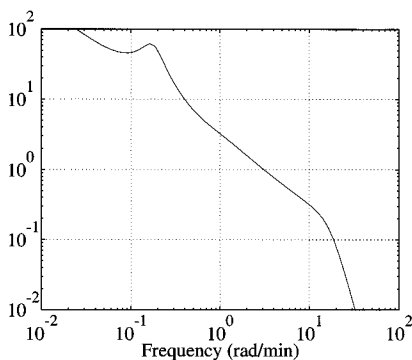


**Figure 6.** Loop gain for the secondary temperature loop  $K_c = 5.53$ .

The loop gain  $L = K_c K_{Tx} g_{x1}$  for the cascade loop with the optimal controller gain  $K_c = 5.53$  is shown in Figure 6. The loop gain crosses 1 in magnitude at frequency  $\omega_c = 3.0$  rad/min, which is the approximate bandwidth of that loop. However, valve dynamics, measurement dynamics, liquid lag from the top to tray 34 of about 0.3 min, etc., probably give that the closed-loop bandwidth must be about 1 rad/min or less. Thus, in practice the controller gain should be reduced by a factor of about 3, and we will use a controller gain  $K_c = 5.53/3 = 1.84$  in the following. This will not seriously impair the “decoupling” property of the secondary loop, as we note from Figure 5 that the RGA plot is rather insensitive to the value of  $K_c$ . Alternatively, we might have introduced dynamics into  $c_x$  to avoid instability from too high loop gain, for example, a PI controller.

No RHP zeros are obtained for the resulting “open-loop” system  $\tilde{G}(s)$  for any value of  $K_c$ .

The “closed-loop” disturbance-rejection properties are also improved through use of the temperature cascade. This is seen from Figure 7 which shows the closed-loop disturbance gain, CLDG =  $G_{\text{diag}} G^{-1} G_d$ , as a function of the secondary controller gain,  $K_c$ , for the most difficult disturbance (effect of  $F$  on  $x_B$ ). All the elements are also shown for the column with a secondary loop with  $K_c = 5.53$ . Note that in the plots the outputs have been scaled such that an output of magnitude 1 corresponds to 0.01 mole fraction units.

The other elements of the CLDG were also improved by the temperature cascade. This is specifically mentioned, as changes to the plant or control system may sometimes improve the disturbance-rejection properties in one measurement at the expense of another. Here, however, disturbance-rejection was improved throughout.

**4.3. Simulations.** Similar results are obtained from Figure 8 which shows a simulation of a step change in the same disturbance. We thus find that closing the

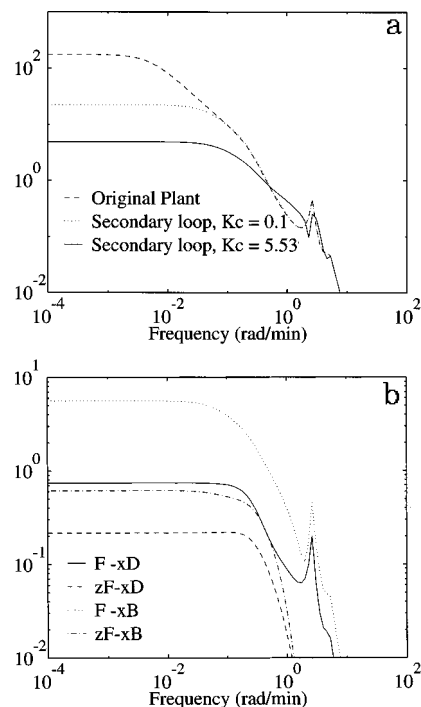


**Figure 7.** Improved disturbance rejection with temperature cascade. Note the different scales in the two plots. (a) CLDG for effect on  $x_B$  of disturbance in feed flow  $F$ . (b) CLDG for column with secondary loop,  $K_c = 5.53$ .

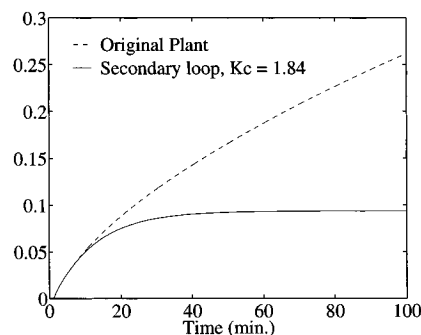


**Figure 8.** Improved open-loop disturbance rejection with temperature cascade,  $K_c = 1.84$ . Plot shows response in  $\Delta x_B$  to a 1% disturbance in the feed rate,  $F$ .

secondary loop strongly reduces the sensitivity of the bottom composition to disturbances. The reason is, of course, that the compositions inside the column are strongly coupled, and fixing the composition at one point results in small changes also at other locations. Especially for a binary separation, temperature is a direct measure of composition. This is important because there is then less need to use fast control in the primary composition loops, and fast control in the primary loops is often impossible because of long measurement delays.

Closed-loop simulations with also the two primary composition loops closed are even more interesting. A measurement delay of  $\Theta = 6$  min for the compositions is used in both loops. For the original plant without the secondary temperature loop we use PID tunings from Skogestad and Lundström (1990):

loop	$K$	$\tau_I$	$\tau_D$
$x_D$	0.14	16.6	3.17
$x_B$	0.12	14.3	3.54

(20)

For the case with a secondary temperature loop we use

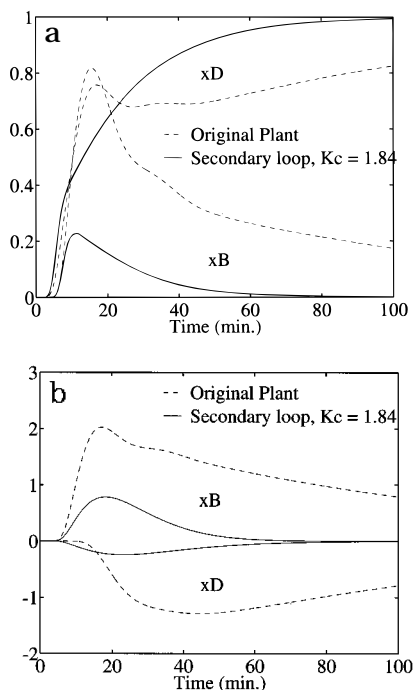


**Figure 9.** Time simulations with composition loops closed. (a) Response to a setpoint change in distillate;  $\Delta x_D = 0.01$  (scaled to 1). (b) Response to a 50% step change in feed rate.

PID tunings based on the Ziegler–Nichols tuning rule but with the proportional gain reduced by a factor of 2 (and, again,  $K_c = 1.84$ ),

loop	$K$	$\tau_I$	$\tau_D$
$x_D$	3.71	6.28	1.57
$x_B$	0.56	6.98	1.75

The temperature measurement in the latter case is passed through the filter

$$f = \frac{1}{1 + \tau_f s} \quad (22)$$

where  $\tau_f = 0.5$  min, to account for some sensor dynamics.

Time simulations with a comparison of the two control systems are given in Figure 9. We see from the simulations that the secondary temperature loop provides for much better control of the top composition,  $x_D$ , with somewhat less improvement for the bottom composition,  $x_B$ . This is as expected since the temperature sensor is located toward the top (stage 34 or stage 8 from the top) and its setpoint is determined by the  $x_D$  controller. In effect we have achieved a one-way decoupling: With  $u_1 = V$  and  $u_{2,x} = T_s$  as the new inputs, we find that  $u_1$  has an effect on  $y_1 = x_B$ , but very little effect on  $y_2 = y_D$ , whereas  $u_{2,x}$  has an effect on  $y_1$  and a somewhat less effect on  $y_2$ .

**4.4. Actuator Behavior.** Including the secondary loop gives larger (and earlier) input signals (changes in reflux and boilup) than for the original plant without compromising stability. This is natural since the decoupling effect of the cascade allows us stable operation without detuning the composition controllers to account for the phase lag contribution of the deadtime  $\Theta$ .

It may be argued that this procedure with a fast secondary loop will produce unrealistically large or oscillatory input signals. There may also exist actuators for which fast operation is not possible, for example,

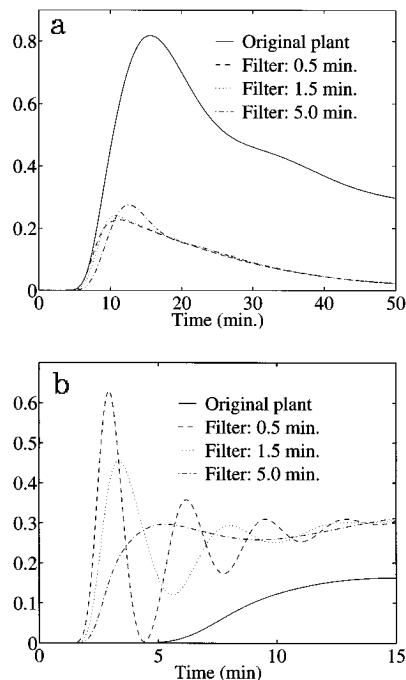


**Figure 10.** Responses to a setpoint change in  $x_D$  ( $\Delta x_D = 0.01$ ) for various filter time constants  $\tau_f$ . (a) Bottoms composition,  $x_B$ . (b) Boilup rate,  $V$ .

when using other process streams as heat sources/sinks. The effect of slower actuators is emulated by increasing the filter time constant  $\tau_f$ . This comparison of actuator speed, not to be mistaken for a design procedure, will show the benefit of even a very slow secondary loop.

The effect of varying the filter time constant  $\tau_f$  is evaluated with respect to composition response and actuator behavior in Figure 10. The figure shows the responses in  $x_B$  and boilup  $V$  to a setpoint change in  $x_D$  for  $\tau_f$  equal to 0.5, 1.5, and 5 min as well as the original plant with no secondary loop. The actuator behavior is significantly different for the varying  $\tau_f$ , with higher  $\tau_f$  (slower secondary loop) giving less vigorous actuator use. However, the composition responses are virtually equal to the system with a short filter time constant with only a minor addition to the initial transients. The limited actuator dynamics does not remove the main effect of the temperature cascade; making the composition responses approximately as fast as the liquid lag  $\Theta_L$  through the column. This is quite readily observed in Figure 10b, where  $V$  in the original plant is delayed by  $\approx \Theta$  before counteracting changes in  $x_D$ . The column with the secondary loop, however, shows changes in  $V$  after  $\approx \Theta_L$ . Deadtime in the secondary loop has been neglected as this would obscure the comparison. Shorter deadtimes than in a composition measurement are, however, anticipated.

The conclusion is that a slower secondary loop will remove actuator oscillations with insignificant performance loss. Tuning of  $K_c$  is easily done online, confirming that removal of oscillations in the secondary loop may be a good starting point for tuning cascade control systems. Tuning of the primary loops based on a fixed  $K_c$  worked well. This solution seems robust to changing  $K_c$  values.

The benefit of including integral action in the secondary loop has also been evaluated, using the controller

$$c(s) = \frac{-1.84}{s}(1 + \tau_i s) \quad (23)$$

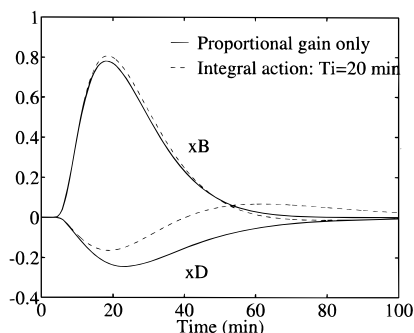


**Figure 11.** Response to a 50% step change in feed rate  $F$  with and without integral action in the secondary loop.

The integral time  $\tau_I$  was kept high (low effect) to reveal primarily marginal effects.

Figure 11 shows the response to a feed rate disturbance when integral action is included in the primary loop. We see that there is some improvement in the distillate composition control, while the overshoot in the bottoms composition becomes slightly worse. The distillate composition also shows a slightly delayed settling. The responses to changes in  $z_F$  and in the setpoints behaved largely in the same manner (not shown); an improvement in one output is balanced by an increased overshoot in the other. There does not seem to be any incentive for including integral action in the secondary loop for this choice of deadtimes and time constants.

## 5. (L/D)(V/B) Configuration

We will now turn our focus to the (L/D)(V/B) configuration, that is, use the ratio between  $L$  and  $D$  to affect the top composition and manipulate the bottoms composition through the ratio between  $V$  and  $B$ . Shinskey (1984) claims that the (L/D)(V/B) configuration is applicable over the broadest range of cases. This configuration has also been recommended by others (e.g., Rademaker, 1975). A drawback is the interdependence between level and composition control and the need for more measurements. This control configuration also depends on fast level control, without which the level and composition control will interact with each other.

The (L/D)(V/B) control scheme generally has lower interaction in terms of RGA or  $\Lambda$  than, for example, the LV configuration. Flow disturbances are also handled well. The reason for this is that the internal flows are adjusted together with the external flows when the level control responds. Despite this, a temperature cascade might be a good investment in order to make the composition control quicker.

When using  $L/D$  and  $V/B$  for control, the following dynamic relations exist between  $L$ ,  $V$ ,  $D$ , and  $B$  and  $L/D$  and  $V/B$  when assuming perfect level control (Skogestad and Morari, 1987)

$$dL = D d\left[\frac{L}{D}\right] + \frac{L}{D} dD \quad (24)$$

$$dV = B d\left[\frac{V}{B}\right] + \frac{V}{B} dB \quad (25)$$

This shows how the level control affects the internal streams and thus the product compositions. For a (diagonal) decentralized controller at a fixed operating point the LV and (L/D)(V/B) configurations are interchangeable through

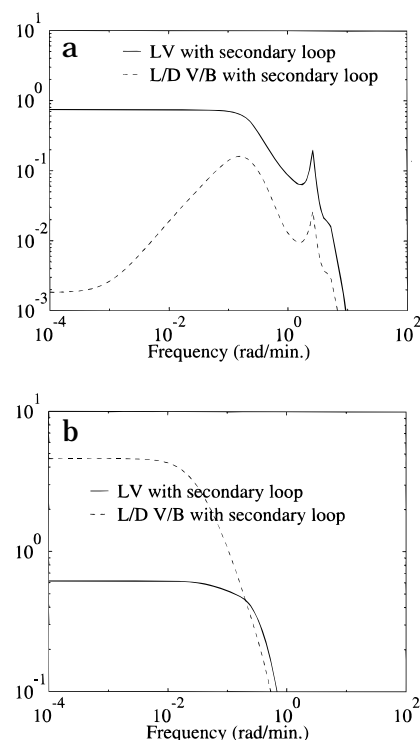


**Figure 12.** Closed-loop disturbance gain of LV and (L/D)(V/B) configurations with secondary loop installed. (a) Effect of feed flow disturbance on top composition,  $x_D$ . (b) Effect of feed composition disturbance on bottom composition,  $x_B$ .

$$du = \begin{bmatrix} dL \\ dV \\ dD \\ dB \end{bmatrix} = \begin{bmatrix} D & 0 & (L/D)K & 0 \\ 0 & B & 0 & (V/B)K \\ 0 & 0 & K & 0 \\ 0 & 0 & 0 & K \end{bmatrix} \begin{bmatrix} dy_D \\ dy_B \\ dM_D \\ dM_B \end{bmatrix} = \Delta dy \quad (26)$$

where  $K$  is the gain in the level control loop, i.e.,  $dD = K dM_D$  and  $dB = K dM_B$ .

The column with the (L/D)(V/B) configuration has  $\lambda_{11}(0) = 3.29$  for the (L/D)(V/B) configuration versus 35.5 for the LV configuration. Applying a secondary control loop makes both schemes one-way interactive at steady state, so a comparison must be based upon other indices. We therefore look at the closed-loop disturbance gain for these two configurations.

The CLDG reveals that the increased handling of flow disturbances of the (L/D)(V/B) configuration is present also with the secondary loop installed. Figure 12 shows how the (L/D)(V/B) configuration is superior toward feed flow changes, while not rejecting feed composition disturbances as well as the LV case. The responses shown are representative also for the two channels not shown.

The results in Figure 12 are confirmed by simulations. Using the same tuning procedure as for the LV case, we get the following controller tunings:

loop	$K$	$\tau_I$	$\tau_D$
$x_D$	1.18	10.5	2.62
$x_B$	0.035	10.5	2.62

Figure 13a shows the improved feed flowrate disturbance handling with the (L/D)(V/B) configuration. The response to a change in  $z_F$  (not shown), on the other hand, gives the opposite conclusion, as predicted by the CLDG. In both cases  $x_B$  is most difficult to control.



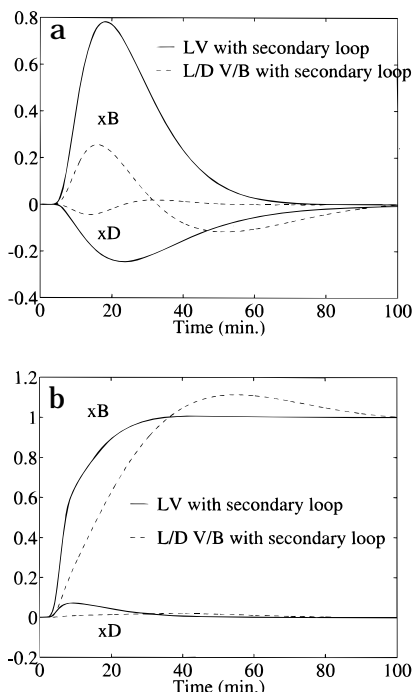


**Figure 13.** Simulations of *LV* and *(L/D)(V/B)* configurations with secondary loop installed. (a) Response to feed flow disturbance. (b) Response to bottom composition setpoint change.

Simulated setpoint changes (as represented by  $x_B$  in Figure 13b) show that the *LV* and *(L/D)(V/B)* configurations behave much more similarly to setpoint changes than toward disturbances. This is reasonable since the interaction properties are almost equal (with a secondary loop) and the change in internal flows will be applied equally fast in both cases.

## 6. Using Two Cascades

Since using an intermediate temperature for composition control works well, why not use this scheme for controlling both top and bottom composition? We choose a tray 8 stages from the bottom ( $N = 8$ ) for the bottom composition control cascade. Denoting the multiple temperature measurements and corresponding gains with the tray number, we get the model:

$$\begin{pmatrix} x_D \\ x_B \\ x_{34} \\ x_8 \end{pmatrix} = \begin{pmatrix} g_{11} & g_{12} \\ g_{21} & g_{22} \\ g_{34,1} & g_{34,2} \\ g_{8,1} & g_{8,2} \end{pmatrix} \begin{pmatrix} L \\ V \end{pmatrix} = \begin{pmatrix} 0.8754 & -0.8618 \\ 1.0846 & -1.0982 \\ 6.3912 & -6.3051 \\ 10.9603 & -11.0723 \end{pmatrix} \begin{pmatrix} L \\ V \end{pmatrix} \quad (28)$$

Using developments similar to those in section 3, we can construct a plant  $\tilde{G}$  such that

$$\begin{pmatrix} x_D \\ x_B \end{pmatrix} = \tilde{G} \begin{pmatrix} T_{34,s} \\ T_{8,s} \end{pmatrix} \quad (29)$$

The elements of  $\tilde{G}$  (which are omitted for brevity) all contain both  $K_1$  and  $K_2$ , the cascade proportional gains in the top and bottom, respectively. The relative gain for this case is  $\lambda_{11} = 1/(1 - Y)$ , where

$$Y = ((g_{21}(1 + K_2 K_{Tx} g_{8,2})K_1 - g_{22}K_2 K_{Tx} g_{8,1}K_1) \times (g_{12}(1 + K_1 K_{Tx} g_{34,1})K - g_{11}K_1 K_{Tx} g_{34,2}K_2)) / ((g_{11}(1 + K_2 K_{Tx} g_{8,2})K_1 - g_{12}K_2 K_{Tx} g_{8,1}K_1) \times (g_{22}(1 + K_1 K_{Tx} g_{34,1})K_2 - g_{21}K_1 K_{Tx} g_{34,2}K_2)) \quad (30)$$

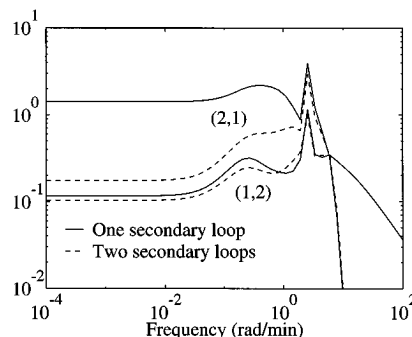


**Figure 14.** Comparison of PRGA with one and two secondary loops installed. Diagonal entries (corresponding to  $\lambda_{11}$ ) are omitted.

Solving for  $K_i$  that will give least interaction ( $\lambda_{11} = 1.0$  or  $Y = 0$  in our sense) yields the following answers:

$$K_1 = K_{Tx}^{-1} \left( \frac{g_{12}}{g_{11}g_{34,2} - g_{12}g_{34,1}} \right) \nabla K_2 \quad (31)$$

$$K_2 = K_{Tx}^{-1} \left( \frac{g_{12}}{g_{11}g_{8,2} - g_{12}g_{8,1}} \right) \nabla K_1$$

We see that there exist multiple solutions for  $K_i$  in this case and that which values to choose is not so obvious. We will here choose  $K_1$  and  $K_2$  from eq 31, corresponding to choosing both  $K_i$  as if the cascades were independent.

The secondary loop gain  $K_1$  is thus chosen equal to the single cascade case ( $K_1 = -1.84$ ). The solution to the bottom secondary controller gives an optimal cascade gain of  $K_2 = 2.94$ . We detune the bottom cascade controller by a factor of 3 for the reasons given earlier, arriving at  $K_2 = 0.98$  for the implemented controller.

At this point it is of interest to see how the *one-way* interaction has changed compared to the single secondary loop case. Figure 14 shows the PRGA (defined in section 3.2) for these two cases. The second secondary loop has reduced the one-way interaction from loop 1 to measurement  $x_B$  significantly. This is in line with the corresponding improvement from the first cascade, which largely improved the interaction properties toward output 1;  $x_D$  (also seen in Figure 14). Both cascades improve the interaction properties of the measurement they are closest to.

Turning toward the disturbance rejection properties, these are only slightly improved over the case with one temperature cascade. From Figure 15 we see that feed flow disturbances have less influence on  $x_B$ , while the other channels are less changed.

Using the given cascade tunings, we then use Ziegler–Nichols tuning rules for the composition loops as described earlier, arriving at

loop	$K$	$\tau_I$	$\tau_D$
$x_D$	2.21	6.54	1.64
$x_B$	1.82	6.16	1.54

(32)

The simulations in Figure 16 show that two temperature cascades generally give a worse performance compared to using one cascade, although there is a small improvement in the initial response of the bottoms composition. This is natural since the first temperature cascade has already stabilized the column profile a great deal and any improvements should come at the end closest to the additional cascade. The overall improve-

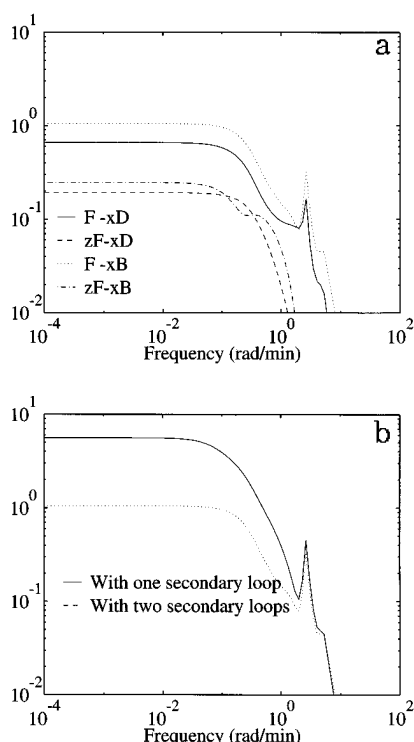


**Figure 15.** Closed-loop disturbance gain for the LV configuration with two secondary loops. (a) Closed-loop disturbance gain. (b) Comparison of worst CLDG element,  $F$  to  $x_B$ , with the single secondary loop case.

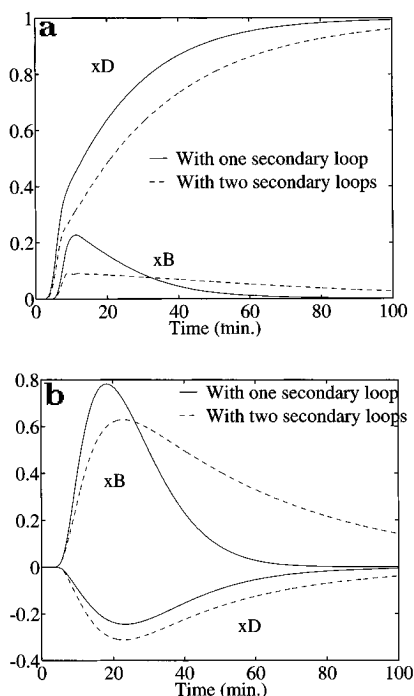


**Figure 16.** Comparison of simulation results with one and two secondary loops. (a) Response to a setpoint change in distillate;  $\Delta x_D = 0.01$ . (b) Response to a 50% step change in feed rate.

ment does, however, not warrant the extra cascade loop in this case.

## 7. Discussion

1. We note from the simulations that the feed flow disturbance  $\Delta F$  has a rather large effect on  $x_B$  even with the secondary loop closed. The reason is that it takes some time before the temperature sensor near the top

registers this disturbance. To improve this response, the temperature sensor should be located in the bottom part of the column. However, in this case the top composition would become more sensitive to disturbances. The obvious conclusion is to place the temperature sensor in the top part (and close this loop using  $L$ ) if the top composition is most critical or place it in the bottom (and close this loop with  $V$ ) if the bottom composition is most critical.

2. A second temperature cascade in two-point distillation control is not advisable from the results shown here.

3. If large variations in the operating point of the column are expected, one may choose to use the weighted average of several tray temperatures for the temperature measurement. This will avoid the problem of an insensitive measurement if the temperature profile becomes flat at the selected tray location. The outer cascade which contains integral action will in any case reset the setpoint of the average temperature to its correct value.

4. The use of "weighted average temperature" is indeed very similar to the static composition estimator of Mejdell. But, as noted before, even with such an estimator, it may be a good idea to implement an independent inner temperature cascade. Also, temperature cascades need not be updated due to the feedback nature.

5. The reason why the temperature cascade reduces interaction is essentially as follows. The distillation column is actually quite decoupled at high frequencies due to the flow dynamics. However, interaction is severe at low frequencies. Therefore, if one can close one loop with sufficiently high gain, one can at least make the system one-way interactive and reduce the RGA also at lower frequencies. It is then possible to implement advanced controllers on top of this without regard for the robustness problems which follow when the RGA is large.

## Nomenclature

$B$  = bottoms flow rate [mol/time]

$c$  = monovariable controller transfer function

$C$  = multivariable controller transfer function

$d$  = disturbance

$D$  = distillate flow rate [mol/time]

$f$  = filter transfer function

$F$  = feed flow rate [mol/time]

$g$  = single plant transfer element

$G$  = plant transfer function

$\tilde{G}$  = plant transfer function with secondary loop closed

$I$  = identity matrix

$K_c$  = Secondary controller gain

$K_{Tx}$  = relation between composition change and temperature change

$L$  = liquid reflux flow rate in top of column [mol/time]

$M$  = molar holdup in condenser and reboiler [mol]

$N$  = tray number

$p$  = pressure

$q$  = enthalpy

$T$  = temperature [ $^{\circ}\text{C}$ ]

$u$  = manipulated input

$V$  = boilup vapor flow rate in bottom of column [mol/time]

$V_T$  = top tray vapor flow rate [mol/time]

$x$  = liquid mole fraction

$y$  = vapor mole fraction

## Greeks

$\alpha$  = relative volatility

$\Lambda, \lambda$  = relative gain array (RGA)

$\tau_f$  = filter time constant

$\Theta$  = deadtime [time]

$\Theta_L$  = liquid lag [time]

### Subscripts

1, 2 = numbering of measurements and manipulated variables = individual transfer functions = multiple secondary controller gains

$ij$  = reference to elements in transfer functions or analysis results

$L, V, D, B$  = flow rates as above

$s$  = temperature setpoint

$x$  = tray number of secondary measurement

$u, y, d$  = reference to manipulated input, measurement, or disturbance

### Literature Cited

- Fagervik, K. C.; Waller, K. V.; Hammarström, L. G. One-way and Two-way Decoupling in Distillation. *Chem. Eng. Commun.* **1981**, *21*, 235.
- Fuentes, C.; Luyben, W. L. Control of High-Purity Distillation Columns. *Ind. Eng. Chem. Process Des. Dev.* **1983**, *22*, 361–366.
- Grosdidier, P.; Morari, M.; Holt, B. R. Closed-Loop Properties from Steady-State Gain Information. *Ind. Eng. Chem. Fundam.* **1985**, *24*, 221–235.
- Hovd, M.; Skogestad, S. Simple Frequency-Dependent Tools for Control System Analysis, Structure Selection and Design. *Automatica* **1992**, *28* (5), 989–996.
- Kister, H. Z. *Distillation Operation*; McGraw-Hill: New York, 1990.
- Krishnaswamey, P. R.; Rangaiah, G. P. Role of Secondary Integral Action in Cascade Control. *Chem. Eng. Res. Eng.* **1992**, *70*, 149–152.

Krishnaswamey, P. R.; Rangaiah, G. P.; Jha, R. K.; Deshpande, P. B. When To Use Cascade Control. *Ind. Eng. Chem. Res.* **1990**, *29*, 2163–2166.

Mejdell, T.; Skogestad, S. Estimation of distillation composition from multiple temperature measurements using PLS regression. *Ind. Eng. Chem. Res.* **1991a**, *30* (12), 2543–2555.

Mejdell, T.; Skogestad, S. Composition estimator in a pilot plant distillation column using multiple temperatures. *Ind. Eng. Chem. Res.* **1991b**, *30* (12), 2555–2564.

Rademaker, O.; Rijnsdorp, J. E.; Maarleveld, A. *Dynamics and Control of Continuous Distillation Units*; Elsevier: Amsterdam, The Netherlands, 1975.

Shinsky, F. G. *Distillation Control*, 2nd ed.; McGraw-Hill: New York, 1984.

Skogestad, S.; Morari, M. Control configuration Selection for Distillation Columns. *AIChE J.* **1987**, *33* (10), 1620–1635.

Skogestad, S.; Morari, M. LV-control of a High-Purity Distillation Column. *Chem. Eng. Sci.* **1988**, *43* (1), 33–48.

Skogestad, S.; Lundström, P. Mu-optimal LV-control of Distillation Columns. *Comput. Chem. Eng.* **1990**, *14* (4/5), 401–413.

Skogestad, S.; Lundström, P.; Jacobsen, E. W. Selecting the best distillation control configuration. *AIChE J.* **1990**, *36* (5), 753–764.

Tolliver, T. L.; McCune, L. C. Finding the Optimum Temperature Control Trays for Distillation Columns. InTech, Sept 1980.

Received for review June 20, 1995

Accepted September 29, 1995<sup>®</sup>

IE940758P

<sup>®</sup> Abstract published in *Advance ACS Abstracts*, December 1, 1995.